

1 Experimental observation of transient $\delta^{18}\text{O}$ interaction between snow and
2 advective airflow under various temperature gradient conditions

3
4 Pirmin Philipp Ebner¹, Hans Christian Steen-Larsen^{2,3}, Barbara Stenni⁴, Martin
5 Schneebeli^{1,*}, and Aldo Steinfeld⁵

6 ¹ *WSL Institute for Snow and Avalanche Research SLF, 7260 Davos Dorf, Switzerland*

7 ² *LSCE Laboratoire des Sciences du Climat et de l'Environnement, Gif-Sur-Yvette Cedex, France*

8 ³ *Center for Ice and Climate, Niels Bohr Institute, University of Copenhagen, Copenhagen, Denmark*

9 ⁴ *Department of Environmental Sciences, Informatics and Statistics, University Ca' Foscari of Venice,*
10 *Venice, Italy*

11 ⁵ *Department of Mechanical and Process Engineering, ETH Zurich, 8092 Zurich, Switzerland*

12
13 **Abstract**

14 Stable water isotopes ($\delta^{18}\text{O}$) obtained from snow and ice samples of polar regions
15 are used to reconstruct past climate variability, but heat and mass transport processes
16 can affect the isotopic composition. Here we present an experimental study on the effect
17 of airflow on the snow isotopic composition through a snow pack in controlled
18 laboratory conditions. The influence of isothermal and controlled temperature gradient
19 conditions on the $\delta^{18}\text{O}$ content in the snow and interstitial water vapor is elucidated. The
20 observed disequilibrium between snow and vapor isotopes led to the exchange of
21 isotopes between snow and vapor under non-equilibrium processes, significantly
22 changing the $\delta^{18}\text{O}$ content of the snow. The type of metamorphism of the snow had a
23 significant influence on this process. These findings are pertinent to the interpretation of
24 the records of stable isotopes of water from ice cores. These laboratory measurements

* Corresponding author. Email: schneebeli@slf.ch

25 suggest that a highly resolved climate history is relevant for the interpretation of the
26 snow isotopic composition in the field.

27

28 *Keywords:* snow, isotope, isothermal, metamorphism, advection, tomography, post-depositional process

29

30 **1. Introduction**

31 Water stable isotopes in polar snow and ice have been used for several decades as
32 proxies for global and local temperatures (e.g. Dansgaard, 1964; Lorius et al., 1979;
33 Grootes et al., 1994; Petit et al., 1999; Johnsen et al., 2001; EPICA Members, 2004).
34 However, the processes that influence the isotopic composition of precipitation in high-
35 latitude are complex, making direct inference of paleo temperatures from the isotopic
36 record difficult (Cuffey et al., 1994; Jouzel et al., 1997, 2003; Hendricks et al., 2000).
37 Several factors affect the vapor and snow isotopic composition, which give rise to ice
38 core isotopic composition, starting from the process of evaporation in the source region,
39 transportation of the air mass to the top of the ice sheet, and post-depositional processes
40 (Craig and Gordon, 1964; Merlivat and Jouzel, 1979; Johnsen et al. 2001; Ciais and
41 Jouzel, 1994; Jouzel and Merlivat, 1984; Jouzel et al., 2003; Helsen et al., 2005, 2006,
42 2007; Cuffey and Steig, 1998; Krinner and Werner, 2003). Mechanical processes such
43 as mixing, seasonal scouring, or spatial redistribution of snow can alter seasonal and
44 annual records (Fisher et al., 1983; Hoshina et al., 2014). Post-depositional processes
45 associated with wind scouring and snow redistribution are known to introduce a “post-
46 depositional noise” in the surface snow. Comparisons of isotopic records obtained from
47 closely located shallow ice cores have allowed for estimation of a signal-to-noise ratio

48 and a common climate signal (Fisher and Koerner, 1988, 1994; White et al., 1997;
49 Steen-Larsen et al., 2011; Sjolte et al., 2011; Masson-Delmotte et al., 2015). After
50 deposition, interstitial diffusion in the firn and ice affects the water-isotopic signal but
51 back-diffusion or deconvolution techniques have been used to establish the original
52 isotope signal (Johnsen, 1977; Johnsen et al., 2000).

53 Snow is a bi-continuous material consisting of fully connected ice crystals and pore
54 space (air) (Löwe et al., 2011). Because of the proximity to the melting point, the high
55 vapor pressure causes a continuous recrystallization of the snow microstructure known
56 as snow metamorphism, even under moderate temperature gradients (Pinzer et al.,
57 2012). The whole ice matrix is continuously recrystallizing by sublimation and
58 deposition, with vapor diffusion as the dominant transport process. Pinzer et al. (2012)
59 showed that a typical half-life of the ice matrix is a few days. The intensity of the
60 recrystallization is dictated by the temperature gradient and this can occur under mid-
61 latitude or polar conditions. Temperature, and geometrical factors (porosity and specific
62 surface area) also play a significant role (Pinzer and Schneebeli, 2009; Pinzer et al.,
63 2012).

64 The interpretation of ice core data and the comparison with atmospheric model
65 results implicitly rely on the assumption that the snowfall precipitation signal is
66 preserved in the snow-ice matrix (Werner et al., 2011). Classically, ice-core stable-
67 isotope records are interpreted as reflecting precipitation-weighted signals, and
68 compared to observations and atmospheric model results for precipitation, ignoring
69 snow-vapor exchanges between surface snow and atmospheric water vapor (e.g. Persson
70 et al., 2011). However, recent studies carried out on top of the Greenland and Antarctic
71 ice sheets combining continuous atmospheric water vapor isotope observations with
72 daily snow surface sampling document a clear day-to-day variation of isotopic

73 composition of surface snow between precipitation events as well as diurnal change in
74 the snow isotopes (Steen-Larsen et al., 2014a; Ritter et al., 2016; Casado et al., 2016).
75 This effect was interpreted as being caused by the uptake of the synoptic-driven
76 atmospheric water-vapor isotope signal by individual snow crystals undergoing snow
77 metamorphism (Steen-Larsen et al., 2014a) and the diurnal variation in moisture flux
78 (Ritter et al., 2016). However, the impact of this process on the isotope-temperature
79 reconstruction is not yet sufficiently understood, but crucial to constrain. This process,
80 compared to interstitial diffusion (Johnsen, 1977; Johnsen et al., 2000), will alter the
81 isotope mean value. The field observations challenge the previous assumption that
82 sublimation occurred molecular layer-by-layer with no resulting isotopic fractionation
83 (Dansgaard, 1964; Friedman et al., 1991; Town et al., 2008; Neumann and Waddington,
84 2004). It is assumed that the solid undergoing sublimation would not be unduly enriched
85 in the heavier isotope species due to the preferential loss of lighter isotopic species to
86 the vapor (Dansgaard, 1964; Friedman et al., 1991). Because self-diffusion in the ice is
87 about three orders of magnitude slower than molecular diffusion in the vapor, the
88 amount of isotopic separation in snow is assumed to be negligible.

89 Snow has a high permeability (Calonne et al., 2012; Zermatten et al., 2014), which
90 facilitates diffusion of gases and, under appropriate conditions, airflow (Gjessing, 1977;
91 Colbeck, 1989; Sturm and Johnson, 1991; Waddington et al., 1996). In a typical
92 Antarctic and Greenland snow profile, strong interactions between the atmosphere and
93 snow occurs, especially in the first 2 m (Neumann and Waddington, 2004; Town et al.,
94 2008), called the convective zone. In the convective zone, air can move relatively freely
95 and therefore exchange between snow and the atmospheric air occurs. Air flowing into
96 the snow reaches saturation vapor pressure nearly instantly through sublimation
97 (Neumann et al., 2008; Ebner et al., 2015a). Models of the influence of the so-called

108 ‘wind pumping’-effect (Fisher et al., 1983; Neumann and Waddington, 2004), in which
109 the interstitial water vapor is replaced by atmospheric air pushed through the upper
110 meters of the snow pack by small-scale high and low pressure areas caused by irregular
111 grooves or ridges formed on the snow surface (dunes and sastrugi), have assumed that
112 the snow grains would equilibrate with the interstitial water vapor on timescales
113 governed by ice self-diffusion. However, no experimental data are available to support
114 this assumption. With this in mind the experimental study presented here is specifically
115 developed to investigate the effect of ventilation inside the snow pack on the isotopic
116 composition. Only conditions deeper than 1 cm inside a snowpack are considered.
117 Previous work showed that (1) under isothermal conditions, the Kelvin effect leads to a
118 saturation of the pore space in the snow but does not affect the structural change (Ebner
119 et al., 2015a); (2) applying a negative temperature gradient along the flow direction
120 leads to a change in the microstructure due to deposition of water molecules on the ice
121 matrix (Ebner et al., 2015b); and (3) a positive temperature gradient along the flow had
122 a negligible total mass change of the ice but a strong reposition effect of water
123 molecules on the ice grains (Ebner et al., 2016). Here, we continuously measured the
124 isotopic composition of an airflow containing water vapor through a snow sample under
125 both isothermal and temperature gradient conditions. Micro computed-tomography
126 (μ CT) was applied to obtain the 3D microstructure and morphological properties of
127 snow.

118 **2. Experimental setup**

119 Isothermal and temperature gradient experiments with fully saturated airflow and
120 defined isotopic composition were performed in a cold laboratory at around $T_{\text{lab}} \approx -15$
121 $^{\circ}\text{C}$ with small fluctuations of ± 0.8 $^{\circ}\text{C}$ (Ebner et al., 2014). Snow produced from de-
122 ionized tap water in a cold laboratory (water temperature: 30 $^{\circ}\text{C}$; air temperature: -20

123 °C) was used for the snow sample preparation (Schleef et al., 2014). The snow was
124 sieved with a mesh size of 1.4 mm into a box, and isothermally sintered for 27 days at -
125 5 °C to increase the strength, in order to prevent destruction of the snow sample due to
126 the airflow, and to evaluate the effect of metamorphism of snow. The morphological
127 properties of the snow are listed in Table 1. The sample holder (diameter 53 mm, height
128 30 mm, 0.066 liter) was filled by a cylinder cut out from the sintered snow. To prevent
129 air flow between snow sample and the sample holder walls, the undisturbed snow disk
130 was filled in at a higher temperature (about -5 °C) and sintering was allowed for about 1
131 h before cooling down and start of the experiment. The setup of Ebner et al. (2014) was
132 modified by additionally inserting a water vapor isotope analyzer (Model: L1102-I
133 Picarro, Inc., Santa Clara, CA, USA) to measure the isotopic ratio $\delta^{18}\text{O}$ of the water
134 vapor contained in the airflow at the inlet and outlet of the sample holder. The
135 experimental setup consisted of three main components (humidifier, sample holder, and
136 the Picarro analyzer) connected with insulated copper tubing and Swagelok fitting (Fig.
137 1). The tubes to the Picarro analyzer were heated to prevent deposition of water vapor
138 and thereby fractionation. The temperature was monitored with thermistors inside the
139 humidifier and at the inlet and outlet of the snow sample. A dry air pressure tank
140 controlled by a mass flow controller (EL-Flow, Bronkhorst) generated the airflow. A
141 humidifier, consisting of a tube (diameter 60 mm, height 150 mm, 0.424 liter volume)
142 filled with crushed ice particles (snow from Antarctica with low $\delta^{18}\text{O}$ composition), was
143 used to saturate the dry air entering the humidifier with water vapor at an almost
144 constant isotopic composition. The air temperature in the humidifier and at the inlet of
145 the snow sample was maintained at the same value (accuracy ± 0.2 K) to limit the
146 influence of variability in absolute vapor pressure and isotopic composition. We
147 measured the $\delta^{18}\text{O}$ of the water vapor produced by the humidifier before and after each

148 experimental run ($\delta^{18}\text{O}_{\text{hum}}$). The outlet flow ($\delta^{18}\text{O}_a$) of the sample holder was
149 continuously measured during the experiment to analyze the temporal evolution of the
150 isotopic signal. All data from the Picarro analyzer were corrected to the humidity
151 reference level using the established instrument humidity-isotope response (Steen-
152 Larsen et al. 2013; 2014b). In addition, VSMOW-SLAP correction and drift correction
153 were performed. We followed the calibration protocol and used the calibration system
154 described in detail by Steen-Larsen et al. (2013; 2014b).

155 The sample holder described by Ebner et al. (2014) was used to analyze the snow by
156 μCT . Tomography measurements were performed with a modified $\mu\text{-CT80}$ (Scanco
157 Medical). The equipment incorporated a microfocus X-ray source, operated at 70 kV
158 acceleration voltage with a nominal resolution of 18 μm . The samples were scanned
159 with 1000 projections per 180° in high-resolution setting, with typical adjustable
160 integration time of 200 ms per projection. The field of view of the scan area was 36.9
161 mm of the total 53 mm diameter, and subsamples with a dimension of $7.2 \times 7.2 \times 7.2$
162 mm^3 were extracted for further processing. The reconstructed μCT images were filtered
163 using a $3 \times 3 \times 3$ median filter followed by a Gaussian filter ($\sigma = 1.4$, support = 3). The
164 Otsu method (Otsu, 1979) was used to automatically perform clustering-based image
165 thresholding to segment the grey-level images into ice and void phase. Morphological
166 properties in the two-phase system were determined based on the exact geometry
167 obtained by the μCT . Tetrahedrons corresponding to the enclosed volume of the
168 triangulated ice matrix surface were applied on the segmented data to determine
169 porosity (ε) and specific surface area (SSA). Opening size distribution operation was
170 applied in the segmented μCT data to extract the mean pore size (d_{mean}). The opening
171 size distribution can be imagined as virtual sieving with different mesh size (Haussener
172 et al., 2012).

173 Three experiments with saturated advective airflow through the snow sample were
174 performed to record the following parameters and analyze their effects: (1) isothermal
175 conditions to analyze the influence of curvature effects (Kaempfer al et., 2007); (2)
176 positive temperature gradient applied to the snow sample where cold air entering the
177 sample is heated while flowing through the sample in order to analyze the influence of
178 sublimation; (3) negative temperature gradient applied to the snow sample where warm
179 air entering the sample is cooled while flowing across the sample, to analyze the
180 influence of net deposition. During the temperature gradient experiments, a temperature
181 difference of 1.4 °C and 1.8 °C was imposed resulting in a gradient of +47 K m⁻¹ and -60
182 K m⁻¹, respectively. The runs were performed at atmospheric pressure and with a
183 volume flow rate of 3.0 liter min⁻¹ corresponding to an average flow speed in the pores
184 of $\approx 30 \text{ mm s}^{-1}$. In wind pumping theory, an airflow velocity of $u_D \approx 10 \text{ mm s}^{-1}$
185 (corresponding Reynolds number $Re \approx 0.65$) was estimated inside the surface snow
186 layers ($d_{\text{mean}} \approx 1 \text{ mm}$) for a high wind speed above the snow surface ($\approx 10 \text{ m s}^{-1}$)
187 (Neumann, 2003). We performed experiments with airflow velocities inside the snow
188 sample of around 30 mm s^{-1} (corresponding Reynolds number $Re = 0.7$), which was a
189 factor three higher than in natural conditions. But looking at the Reynolds number our
190 experiments were in the feasible flow regime (laminar flow) of a natural snow pack. In
191 experiment (2) the outlet temperature and in experiment (3) the inlet and also the
192 humidifier temperature were actively controlled using thermo-electric elements.
193 Variations in temperature of up to $\pm 0.8 \text{ °C}$ were due to temperature fluctuations inside
194 the cold laboratory, leading to slightly variable temperature gradients and mean
195 temperature in experiment (2) and (3). Table 1 presents a summary of the experimental
196 conditions and the morphological properties of the snow samples. At the end of each
197 experiment, the snow sample was cut into five layers of 6 mm height and the isotopic

198 composition of each layer was analyzed to examine the spatial $\delta^{18}\text{O}$ gradient in the
199 isotopic composition of the snow sample.

200 A slight increase with a maximum of 0.7 ‰ of $\delta^{18}\text{O}$ in the water vapor produced by
201 the humidifier was observed in experiment (1), with lower increases during experiments
202 (2) and (3) (Table 2). This change of $\sim 0.7\text{‰}$ is not significant compared to the
203 difference between the isotopic composition of the water vapor and the snow sample in
204 the sample holder of $\sim 53\text{‰}$ and the temporal change of the water vapor isotopes on the
205 back side of the snow sample.

206 In the first approximately 30 min, the isotopic composition of the measured outflow
207 air $\delta^{18}\text{O}_a$ increased from a low $\delta^{18}\text{O}$ to a starting value of around -29‰ in each
208 experiment. This was due to memory effect possible condensed water left in the tubes
209 from a prior experiment.

210 **3. Results**

211 **3.1 Isothermal condition**

212 The experiment (1) was performed for 24 h at a mean temperature of $T_{\text{mean}} = -15.5$
213 $^{\circ}\text{C}$. $\delta^{18}\text{O}_a$ decreased exponentially in the outlet flow observed throughout the
214 experimental run as shown in Fig. 2. Initially, the $\delta^{18}\text{O}_a$ content in the flow was -27.7‰
215 and exponentially decreased to -47.6‰ after 24 h. The small fluctuations in the $\delta^{18}\text{O}_a$
216 signal at $t \approx 7$ h, 17 h and 23 h were due to small temperature changes in the cold
217 laboratory.

218 We observed a strong interaction between the airflow and the snow as manifest by
219 the isotopic composition of the snow. The $\delta^{18}\text{O}_s$ signal in the snow decreased by 4.75 –
220 7.78 ‰ and an isotopic gradient in the snow was observed after the experimental run,
221 shown in Fig. 3. Initially, the snow had a homogeneous isotopic composition of $\delta^{18}\text{O}_s =$

222 -10.97 ‰ but post-experiment sampling showed a decrease in the snow $\delta^{18}\text{O}$ at the inlet
223 side to -17.75 ‰ and at the outlet side to -15.72 ‰. The spatial $\delta^{18}\text{O}_s$ gradient of the
224 snow had an approximate slope of 0.68 ‰ mm^{-1} at the end of the experimental run.
225 Table 2 shows the $\delta^{18}\text{O}$ value in snow at the beginning ($t = 0$) and end ($t = 24 \text{ h}$) of the
226 experiment.

227 **3.2 Air warming by a positive temperature gradient along the airflow**

228 The experiment (2) was performed over a period of 24 h with an average
229 temperature gradient of approximately $+47 \text{ K m}^{-1}$ (warmer temperatures at the outlet
230 of the snow) and an average mean temperature of -14.7 °C . As in the isothermal
231 experiment (1), we observed a relaxing exponential decrease of $\delta^{18}\text{O}_a$ in the outlet flow
232 throughout the measurement period as shown in Fig. 2, but the decrease was slower
233 compared to the isothermal run. Initially, the $\delta^{18}\text{O}_a$ content in the flow coming through
234 the snow disk was -29.8 ‰ and exponentially decreased to -41.9 ‰ after 24 h. The
235 small fluctuations in the $\delta^{18}\text{O}_a$ signal at $t \approx 2.7 \text{ h}$, and 12.7 h were due to small
236 temperature changes in the cold laboratory.

237 The $\delta^{18}\text{O}_s$ signal in the snow decreased $4.66 - 7.66 \text{ ‰}$ and a gradient in the isotopic
238 composition of the snow was observed after the experimental run, shown in Fig. 3.
239 Initially, the snow had a homogeneous isotopic composition of $\delta^{18}\text{O}_s = -11.94 \text{ ‰}$, but
240 post-experiment sampling showed a decrease at the inlet side to -19.6 ‰ and at the
241 outlet side to -16.6 ‰ . The spatial $\delta^{18}\text{O}_s$ gradient of the snow had an approximate slope
242 of 1.0 ‰ mm^{-1} at the end of the experimental run. Table 2 shows the $\delta^{18}\text{O}_s$ value in
243 snow at the beginning ($t = 0$) and end ($t = 24 \text{ h}$) of the experiment.

244 **3.3 Air cooling by a negative temperature gradient along the air flow**

245 The experiment (3) was performed for 84 h instead of 24 h to better estimate the
246 trend in $\delta^{18}\text{O}_a$ in the outlet flow. An average temperature gradient of approximately -60
247 K m^{-1} (colder temperatures at the outlet of the snow) and an average mean temperature
248 of -13.2 °C were observed during the experiment. As in the previous experiments, a
249 relaxing exponential decrease of $\delta^{18}\text{O}_a$ in the outlet flow was observed throughout the
250 experimental run as shown in Fig. 2, but the decrease was slower compared to the
251 isothermal run and temperature gradient opposed to the airflow. Initially, the $\delta^{18}\text{O}_a$
252 content in the flow was -29.8 ‰ and exponentially decreased to -37.7 ‰ after 84 h. The
253 small fluctuations in the $\delta^{18}\text{O}_a$ signal at $t \approx 7.3$ h, 21.3 h, 31.3 h, 45.3 h, 55.3 h, 69.3 h,
254 and 79.3 h were due to small temperature changes in the cold laboratory.

255 The $\delta^{18}\text{O}_s$ signal in the snow decreased 4.46 – 15.09 ‰ and a gradient in the isotopic
256 composition of the snow was observed after the experimental run, shown in Fig. 3.
257 Initially, the snow had an isotopic composition of $\delta^{18}\text{O}_s = -10.44$ ‰ but post-experiment
258 sampling showed a decrease at the inlet side to -25.53 ‰ and at the outlet side to -15.00
259 ‰. The spatial $\delta^{18}\text{O}_s$ gradient of the snow had an approximate slope of 3.5 ‰ mm^{-1} at
260 the end of the experimental run. Table 2 shows the $\delta^{18}\text{O}_s$ value in snow at the beginning
261 ($t = 0$) and end ($t = 84$ h) of the experiment.

262 **4. Discussion**

263 All experiments showed a strong exchange in $\delta^{18}\text{O}$ between the snow and water-
264 vapor saturated air resulting in a significant change of the value of the stable isotopes in
265 the snow. The advective conditions in the experiments were comparable with surface
266 snow layers in Antarctica and Greenland, but at higher temperature, especially
267 compared to interior Antarctica.

268 The results also showed strong interactions in $\delta^{18}\text{O}$ between snow and air depending
269 on the different temperature gradient conditions. The experiments indicate that

270 temperature variation and airflow above and through the snow structures (Sturm and
271 Johnson, 1991; Colbeck, 1989; Albert and Hardy, 1995) seem to be dominant processes
272 affecting water stable isotopes of surface snow. The results also support the statement
273 that an interplay between theoretically expected layer-by-layer sublimation and
274 deposition at the ice-matrix surface and the isotopic content evolution of snow cover
275 due to mass exchange between the snow cover and the atmosphere occurs (Sokratov and
276 Golubev, 2009). The specific surface area of snow exposed to mass exchange (Horita et
277 al., 2008) and by the depth of the snow layer exposed to the mass exchange with the
278 atmosphere (He and Smith, 1999) plays an important role. Our results support the
279 interpretation that changes in surface snow isotopic composition are expected to be
280 significant if large day-to-day surface changes in water vapor occur in between
281 precipitation events, wind pumping is efficient and snow metamorphism is enhanced by
282 temperature gradients in the upper first centimeters of the snow (Steen-Larsen et al.,
283 2014a).

284 We expect that our findings will lead to improvement of the interpretation of the
285 water stable isotope records from ice cores. Classically, ice core stable isotope records
286 are interpreted as paleo-temperature reflecting precipitation-weighted signals. When
287 comparing observations and atmospheric model results for precipitation with ice core
288 records, such vapor-snow exchanges are normally ignored (e.g. Persson et al., 2011;
289 Fujita and Abe, 2006). However, vapor-snow exchange enhanced by recrystallization
290 rate seems to be an important factor for the high variation in the snow surface $\delta^{18}\text{O}$
291 signal as supported by our experiments. It was hypothesized that the changes in the
292 snow-surface $\delta^{18}\text{O}$ reported by Steen-Larsen et al. (2014a) are caused by changes in
293 large-scale wind and moisture advection of the atmospheric water vapor signal and

294 snow metamorphism. The strong interaction between atmosphere and near-surface snow
295 can modify the ice core water stable isotope records.

296 The rate-limiting step for isotopic exchange in the snow is isotopic equilibration
297 between the pore-space vapor and surrounding ice grains. The relaxing exponential
298 decrease of $\delta^{18}\text{O}$ in the outflow of our experiments predicted that full isotopic
299 equilibrium between snow and atmospheric vapor will not be reached at any depth
300 (Waddington et al., 2002; Neumann and Waddington, 2004) but changes towards
301 equilibrium with the atmospheric state occurs (Steen-Larsen et al., 2013, 2014a).

302 As snow accumulates, the upper 2 m are advected through the ventilated zone
303 (Neumann and Waddington, 2004; Town et al., 2008). In areas with high accumulation
304 rate (e.g. South Greenland), snow is advected for a short time through the ventilated
305 zone. The snow exposed a relatively short time to vapor snow exchange would result in
306 higher spatial variability compared to long-time exposure. However, the effects of snow
307 ventilation on isotopic composition may become more important as the accumulation
308 rate of the snow decreases ($< 50 \text{ mm a}^{-1}$), such that snow remains in the near-surface
309 ventilated zone for many years (Waddington et al., 2002; Hoshina et al., 2014; Hoshina
310 et al., 2016). As the snow remains longer in the near-surface ventilated zone, a larger
311 $\delta^{18}\text{O}$ exchange between snow and atmospheric vapor will occur. Consequently, the
312 isotopic content of layers at sites with high and low accumulation rates can evolve
313 differently, even if the initial snow composition had been equal, and the sites had been
314 subjected to the same histories of air-mass vapor.

315 Despite a relatively small change in the difference between the isotopic composition
316 of the incoming vapor and the snow, large differences in the isotopic composition of the
317 water vapor at the outlet flow exist for the three different experimental setups. Based on
318 the difference in the outlet water vapor isotopic composition, we hypothesized that

319 different processes are at play for the different experiments. It is obvious that there is a
 320 fast isotopic exchange with the surface of the ice crystals, and a much slower timescale
 321 on which the interior of the ice crystals is altered. Due to the low diffusivity of H_2^{16}O
 322 and H_2^{18}O in ice ($D_{\text{H}_2^{18}\text{O}} \approx D_{\text{H}_2^{16}\text{O}} = \sim 10^{-15} \text{ m}^2 \text{ s}^{-1}$ (Ramseier, 1967; Johnsen et al., 2000),
 323 we assumed that the interior of the ice crystals is not altered on the timescale of the
 324 experiment. This explained why the net isotopic change of the bulk sample is relatively
 325 small compared to the changes in the outlet water vapor isotopes. The effective ‘ice-
 326 diffusion depth’ of the isotopic exchange during the experiments is given as $L_D = \sqrt{D \cdot t}$,
 327 where D is the diffusion coefficient of H_2^{16}O and H_2^{18}O in ice, respectively, and t the
 328 experimental time. The calculated ‘ice-diffusion depth’ L_D , is $\sim 9.3 \mu\text{m}$ for experiments
 329 (1) and (2), and $\sim 17.4 \mu\text{m}$ for experiment (3), respectively, indicating an expected a
 330 minimal change of the interior of the ice crystal. However, snow has a large specific
 331 surface area and therefore a high exchange area. This has an effect on the $\delta^{18}\text{O}$ snow
 332 concentration. The fraction of the total volume V_{tot} of ice that is close enough to the ice
 333 surface to be affected by diffusion in time t is then $\rho_{\text{ice}} \cdot \text{SSA} \cdot L_D$, where SSA is the
 334 specific surface area (area per unit mass), and L_D is the diffusion depth, defined above,
 335 for time t . For $t \approx 24$ hours, a large fraction (24 to 43 %) of the total volume V_{tot} of the
 336 ice matrix can be accessed through diffusion. It is quite hard to see the total $\delta^{18}\text{O}$ snow
 337 difference between experiments (1) and (2) after the experiment compared to the $\delta^{18}\text{O}$
 338 of the vapor in the air at the outlet. There is a small, but notable, difference in the total
 339 $\delta^{18}\text{O}$ of the snow between experiment (1) and (2). Due to the higher recrystallization
 340 rate of experiment (2) the spatial $\delta^{18}\text{O}_s$ gradient of the snow (1.0 ‰ mm^{-1}) is higher than
 341 for experiment (1) (0.68 ‰ mm^{-1}). Increasing the experimental time, the $\delta^{18}\text{O}$ change in
 342 the snow increases (experiment (3)). In general, the calculated ‘ice-diffusion depth’ is
 343 realistic under isothermal conditions where diffusion processes are the main factors

344 (Kaempfer and Schneebeli, 2007; Ebner et al., 2015). Applying a temperature gradient,
345 the impact of diffusion is suppressed due to the high recrystallization rate by
346 sublimation and deposition. Due to the low half-life of the ice matrix of a few days, the
347 growth rates are typically on the order of 100 μm per day (Pinzer et al., 2012).
348 Therefore, this redistribution of ice caused by temperature gradient counteracts the
349 diffusion into the solid ice.

350 By comparing similarities and differences between the outcomes of the three
351 experimental setups we will now discuss the physical processes influencing the
352 interaction and exchange processes within the snowpack between the snow and the
353 advected vapor. We first notice that the final snow isotopic profile of experiment (1)
354 (isothermal) and (2) (positive temperature gradient along the direction of the flow) are
355 comparable to each other. Despite this similarity, the evolution in the outlet water vapor
356 of experiment (1) showed a significantly stronger depletion compared to experiment (2).
357 For experiment (3) (negative temperature gradient along the direction of the flow) we
358 observed the smallest change in outlet water vapor isotopes but the largest snow-pack
359 isotope gradient after the experiment. However, this change was caused by 84 hours
360 flow instead of 24 hours.

361 Curvature effects, temperature gradients and therefore the recrystallization rate
362 influence the mass transfer of $\text{H}_2^{16}\text{O}/\text{H}_2^{18}\text{O}$ molecules. The higher the recrystallization
363 rate of the snow the slower the adaption of the outlet air concentration to the inlet air
364 concentration (see in experiment (2) and (3)). Under isothermal conditions (experiment
365 (1)) the only effect influencing the recrystallization rate is the curvature effect
366 (Kaempfer and Schneebeli, 2007). However, based on the experimental observations
367 (Kaempfer and Schneebeli, 2007) this effect decreases with decreasing temperature and
368 increasing experimental time. Applying an additional temperature gradient on a snow

369 sample causes complex interplays between local sublimation and deposition on surfaces
370 and the interaction of water molecules in the air with the ice matrix due to changing
371 saturation conditions of the airflow. Therefore, the recrystallization rate increases and
372 causes the change in the $\delta^{18}\text{O}$ of the air. For experiment (2) there is a complex interplay
373 between sublimation and deposition of water molecules into the interstitial flow (Ebner
374 et al., 2015c) while for experiment (3) there is deposition of molecules carried by the
375 interstitial flow onto the snow crystals (Ebner et al., 2015b). Furthermore, in the
376 beginning of each experiment there is a tendency to sublimate from edges of the
377 individual snow crystals due to the higher curvature. As the edges were sublimated and
378 deposition occurred in the concavities, the individual snow crystals became more
379 rounded, slowing down the transfer of water molecules into the interstitial airflow. We
380 noticed for all three experiments that within the uncertainty of the isotopic composition
381 of the snow, the initial isotopic composition of the vapor was the same and in isotopic
382 equilibrium with the snow. The difference between experiment (1) and (2) lies in the
383 fact that due to the temperature gradient in experiment (2) there is an increased transfer
384 of water vapor with the isotopic composition of the snow into the airflow. Hence the
385 depleted air from the humidifier advected through the snow disk is mixed with a
386 relatively larger vapor flux from the snow crystals. Additionally, we also expected less
387 deposition into the concavities in experiment (2) compared to experiment (1). However,
388 it is interesting to note that the final isotopic profile of the snow disk is similar in
389 experiment (1) and experiment (2). We interpreted this as being a result of two
390 processes acting in opposite direction: although relatively isotope-depleted vapor from
391 the humidifier was deposited on the ice matrix there was also a higher amount of
392 sublimation of relatively isotope-enriched vapor from the snow disk in experiment (2).
393 Experiment (3) separates itself from the other two experiments in the way that as the

394 water vapor from the humidifier is advected through the snow disk there is a continuous
395 deposition of very depleted air due the negative temperature gradient. As for the case of
396 experiment (1) and (2) there was also in experiment (3) a constant sublimation of the
397 convexities into the vapor stream. We notice that despite the fact that experiment (3) ran
398 for 84 hours the snow at the outlet side of the snow-disk did not become more
399 isotopically depleted compared to experiment (1) and (2). However, the snow on the
400 inlet side became significantly more isotopically depleted. This observation, together
401 with the fact that the vapor of the outlet of the snow-disk is less depleted compared to
402 experiment (1) and (2), leads us to hypothesize that there is a relatively larger deposition
403 of isotopically depleted vapor from the humidifier as the vapor is advected through the
404 snow disk. This means that a relatively larger component of the isotopic composition of
405 the vapor is originating by sublimation from the convexities of the snow disk and less
406 from the isotopically depleted vapor from the humidifier.

407 Our results and conclusions indicate that there is a need for additional validation.
408 Specifically, it would be crucial to know the mass balance of the snow disk more
409 precisely, which could be done by reconstructing the entire snow disk following the
410 change in density and morphological properties over the entire height. Ideally, the entire
411 sample would be tomographically measured with a resolution of $4 \times 4 \times 4 \text{ mm}^3$, each
412 cube corresponding to the representative volume. Insights would also be achieved with
413 experiments using snow of the same isotopic composition, but different SSA, as more
414 precise calculation of the different observed exchange rates would be allowed.
415 Additionally, different and colder background temperatures should be tested to better
416 understand inland Antarctic environment and the effect of the quasi-liquid layer, which
417 is necessary for the development of a numerical model. Isotopically different
418 combinations of vapor and snow should be performed. In the present manuscript, vapor

419 with low $\delta^{18}\text{O}$ isotopic composition was transported through snow with relative high
420 $\delta^{18}\text{O}$ isotopic composition. It would be interesting to reverse the combination and
421 perform experiments with different combinations to provide more insights on mass and
422 isotope exchanges between vapor and snow. Experiments with longer running time help
423 to understand the change in the ice matrix better under low accumulation conditions.

424 **4. Summary and conclusion**

425 Laboratory experimental runs were performed where a transient $\delta^{18}\text{O}$ interaction
426 between snow and air was observed. The airflow altered the isotopic composition of the
427 snowpack and supports an improved climatic interpretation of ice core stable water
428 isotope records. The water vapor saturated airflow with an isotopic difference of up to
429 55‰ changed within 24 h and 84 h the original $\delta^{18}\text{O}$ isotope signal in the snow by up to
430 7.64 ‰ and 15.06 ‰. The disequilibrium between snow and air isotopes led to the
431 observed exchange of isotopes, the rate depending on the temperature gradient
432 conditions. Concluding, increasing the recrystallization rate in the ice matrix causes the
433 temporal change of the $\delta^{18}\text{O}$ concentration at the outflow to decrease (experiment (2)
434 and (3)). Decreasing the recrystallization rate causes the temporal curve of the outlet
435 concentration to become steeper reaching the $\delta^{18}\text{O}$ inlet concentration of the air faster
436 (experiment (1)).

437 Additionally, the complex interplay of simultaneous diffusion, sublimation and
438 deposition due to the geometrical complexity of snow has a strong effect on the $\delta^{18}\text{O}$
439 signal in the snow and cannot be neglected. A temporal signal can be superimposed on
440 the precipitation signal, (a) if the snow remains near the surface for a long time, i.e. in a
441 low-accumulation area, and (b) is exposed to a history of air masses carrying vapor with
442 a significantly different isotopic signature than the precipitated snow.

443 These are novel measurements and will therefore be important as the basis for
444 further research and experiments. Our results represent direct experimental observation
445 of the interaction between the water isotopic composition of the snow, the water vapor
446 in the air and recrystallization due to temperature gradients. Our results demonstrate that
447 recrystallization and bulk mass exchange must be incorporated into future models of
448 snow and firn evolution. Further studies are required on the influence of temperature
449 and airflow as well as snow microstructure on the mass transfer phenomena for
450 validating the implementation of stable water isotopes in snow models.

451

452

453 **Acknowledgements**

454 The Swiss National Science Foundation granted financial support under project Nr.
455 200020-146540. H.C. Steen-Larsen was supported by the AXA Research Fund. The
456 authors thank K. Fujita, E. D. Waddington and an anonymous reviewer for the
457 suggestions and critical review. M. Jaggi, S. Grimm, A. Schlumpf, and S. Berben gave
458 technical support. The data for this paper are available by contacting the corresponding
459 author.

460

461 **References**

462 Albert M. R. and Hardy J. P.: Ventilation experiments in a seasonal snow cover, in
463 Biogeochemistry of Seasonally Snow-Covered Catchments, IAHS Publ. 228, edited
464 by K. A. Tonnessen, M. W. Williams, and M. Tranter, 41–49, IAHS Press,
465 Wallingford, UK, 1995.

466 Calonne N., Geindreau C., Flin F., Morin S., Lesaffre B., Rolland du Roscoat S., and
467 Charrier P.: 3-D image-based numerical computations of snow permeability: links

468 to specific surface area, density, and microstructural anisotropy, *The Cryosphere*, 6,
469 939-951, 2012.

470 Casado M., Landais A., Masson-Delmotte V., Genthon C., Kerstel E., Kassi S., Arnaud
471 L., Picard G., Prie F., Cattani O., Steen-Larsen H. C., Vignon E., and Cermak P.:
472 Continuous measurements of isotopic composition of water vapour on the East
473 Antarctic Plateau, *Atmos. Chem. Phys. Discuss.*, doi:10.5194/acp-2016-8, in
474 review, 2016.

475 Ciais P., and Jouzel J.: Deuterium and oxygen 18 in precipitation: Isotopic model,
476 including mixed-cloud processes, *Journal of Geophysical Research*, 99, 16793–
477 16803, doi:10.1029/94JD00412, 1994.

478 Colbeck S. C.: Air movement in snow due to windpumping, *Journal of Glaciology*, 35,
479 209–213, 1989.

480 Craig H. and Gordon L. I.: Deuterium and oxygen 18 variations in the ocean and marine
481 atmosphere, In *proc. Stable Isotopes in Oceanographic Studies and*
482 *Paleotemperatures*, (ed. E. Toniorgi), Spoleto, Italy, 9–130, 1964.

483 Cuffey K. M. and Steig E. J.: Isotopic diffusion in polar firn: Implications for
484 interpretation of seasonal climate parameters in ice-core records, with emphasis on
485 central Greenland, *Journal of Glaciology*, 44, 273–284, 1998.

486 Cuffey K. M., Alley R. B., Grootes P. M., Bolzan J. M., and Anandakrishnan S.:
487 Calibration of the Delta-O-18 isotopic paleothermometer for central Greenland,
488 using borehole temperatures, *Journal of Glaciology*, 40, 341–349, 1994.

489 Dansgaard W.: Stable isotopes in precipitation, *Tellus*, 16, 436–468, 1964.

490 Ebner P. P., Grimm S., Schneebeli M., and Steinfeld A.: An instrumented sample holder
491 for time-lapse micro-tomography measurements of snow under advective

492 conditions, *Geoscientific Instrumentation Methods and Data Systems*, 3, 179–185,
493 doi:10.5194/gi-3-179-2014, 2014.

494 Ebner P. P., Schneebeli M., and Steinfeld A. Tomography-based observation of
495 isothermal snow metamorphism under advective conditions, *The Cryosphere*, 9,
496 1363–1371, 2015a.

497 Ebner P. P., Andreoli C., Schneebeli M., and Steinfeld A.: Tomography-based
498 characterization of ice-air interface dynamics of temperature gradient snow
499 metamorphism under advective conditions, *Journal of Geophysical Research*,
500 *Journal of Geophysical Research Earth Surface*, 120, doi:10.1002/2015JF003648,
501 2015b.

502 Ebner P. P., Schneebeli M., and Steinfeld A.: Metamorphism during temperature
503 gradient with undersaturated advective airflow in a snow sample, *The Cryosphere*,
504 10, 791-797, 2016.

505 EPICA Members: Eight glacial cycles from an Antarctic ice core, *Nature*, 429, 623–
506 628, doi:10.1038/nature02599, 2004.

507 Gjessing Y. T.: The filtering effect of snow, in: *Isotopes and Impurities in Snow and Ice*
508 *Symposium*, edited by: Oeschger, H., Ambach, W., Junge, C. E., Lorius, C., and
509 Serebryanny, L., IASHAISH Publication, Dorking, 118, 199–203, 1977.

510 Grootes P. M., Steig E., and Stuiver M.: Taylor Ice Dome study 1993-1994: An ice core
511 to bedrock, *Antarctic Journal U.S.*, 29, 79–81, 1994.

512 Fisher D. A., Koerner R. M., Paterson W. S. B., Dansgaard W., Gundestrup N., and
513 Reeh N.: Effect of wind scouring on climatic records from ice-core oxygen-isotope
514 profiles, *Nature*, 301, 205–209, doi:10.1038/301205a0, 1983.

515 Fisher D. A. and Koerner R.: The effect of wind on $\delta(18O)$ and accumulation given an
516 inferred record of seasonal δ amplitude from the Agassiz ice cap, Ellesmere island,
517 Canada, *Annals of Glaciology*, 10, 34–37, 1988.

518 Fisher D. A. and Koerner R.: Signal and noise in four ice-core records from the Agassiz
519 ice cap, Ellesmere Island, Canada: Details of the last millennium for stable
520 isotopes, melt and solid conductivity, *The Holocene*, 4, 113–120,
521 doi:10.1177/095968369400400201, 1994.

522 Friedman I., Benson C., and Gleason J.: Isotopic changes during snow metamorphism,
523 in *Stable Isotope Geochemistry: A Tribute to Samuel Epstein*, edited by J. R.
524 O'Neill and I. R. Kaplan, pp. 211–221, Geochemical Society, Washington, D. C.,
525 1991.

526 Haussener S., Gergely M., Schneebeli M., and Steinfeld A.: Determination of the
527 macroscopic optical properties of snow based on exact morphology and direct pore-
528 level heat transfer modeling, *Journal of Geophysical Research*, 117, 1–20,
529 doi:10.1029/2012JF002332, 2012.

530 He H. and Smith R. B.: An advective-diffusive isotopic evaporation-condensation
531 model, *Journal of Geophysical Research*, 104, 18619–18630,
532 doi:10.1029/1999JD900335, 1999.

533 Helsen M. M., van de Wal R. S. W., van den Broeke M. R., van As D., Meijer H. A. J.,
534 and Reijmer C. H.: Oxygen isotope variability in snow from western Dronning
535 Maud Land, Antarctica and its relation to temperature, *Tellus*, 57, 423–435, 2005.

536 Helsen M. M., van de Wal R. S. W., van den Broeke M. R., Masson-Delmotte V.,
537 Meijer H. A. J., Scheele M. P., and Werner M., Modeling the isotopic composition
538 of Antarctic snow using backward trajectories: Simulation of snow pit records,
539 *Journal of Geophysical Research*, 111, doi:10.1029/2005JD006524, 2006.

540 Helsen M. M., van de Wal R. S. W., and van den Broeke M. R.: The isotopic
541 composition of present-day Antarctic snow in a Lagrangian simulation, *Journal of*
542 *Climate*, 20, 739–756, 2007.

543 Hendricks M. B., DePaolo D. J., and Cohen R. C.: Space and time variation of $\delta^{18}\text{O}$ and
544 δD in precipitation: Can paleotemperature be estimated from ice cores?, *Global*
545 *Biogeochemical Cycles*, 14, 851–861, doi:10.1029/1999GB001198, 2000.

546 Horita J., Rozanski K., and Cohen S.: Isotope effects in the evaporation of water: a
547 status report of the Craig-Gordon model, *Isotopes in Environmental Health Studies*,
548 44, 23–49, doi:10.1080/10256010801887174, 2008.

549 Hoshina Y., Fujita K., Nakazawa F., Iizuka Y., Miyake T., Hirabayashi M., Kuramoto
550 T., Fujita S., and Motoyama H.: Effect of accumulation rate on water stable
551 isotopes of near-surface snow in inland Antarctica. *Journal of Geophysical*
552 *Research - Atmospheres*, 119(1), 274–283. doi:10.1002/2013JD020771, 2014.

553 Hoshina Y., Fujita K., Iizuka Y., Motoyama H.: Inconsistent relations among major ions
554 and water stable isotopes in Antarctica snow under different accumulation
555 environments. *Polar Science*, 10, doi:10.1016/j.polar.2015.12.003, 2016.

556 Johnsen S. J.: Stable isotope homogenization of polar firn and ice, in *Isotopes and*
557 *Impurities in Snow and Ice*, Proceeding of the Grenoble Symposium,
558 August/September 1975, 210–219, IAHS AISH Publication, 118, Grenoble, France,
559 1997.

560 Johnsen S. J., Clausen H. B., Cuffey K. M., Hoffman G., Schwander J., and Creyts T.:
561 Diffusion of stable isotopes in polar firn and ice: The isotope effect in firn
562 diffusion, in *Physics of Ice Core Records*, edited by T. Hondoh, 121–140,
563 Hokkaido University Press, Sapporo, Japan, 200.

564 Johnsen S. J., Dahl-Jensen D., Gundestrup N., Steffensen J. P., Clausen H. B., Miller
565 H., Masson-Delmotte V., Sveinbjörnsdóttir A. E., and White J.: Oxygen isotope
566 and palaeotemperature records from six Greenland ice-core stations: Camp
567 Century, DYE-3, GRIP, GISP2, Renland and NorthGRIP, *Journal of Quaternary*
568 *Science*, 16, 299–307, doi:10.1002/jqs.622, 2001.

569 Jouzel J. and Merlivat L.: Deuterium and oxygen 18 in precipitation: Modeling of the
570 isotopic effects during snow formation, *Journal of Geophysical Research*, 89,
571 11749–11757, doi:10.1029/JD089iD07p11749, 1984.

572 Jouzel J., Merlivat L., Petit J. R., and Lorius C.: Climatic information over the last
573 century deduced from a detailed isotopic record in the South Pole snow, *Journal of*
574 *Geophysical Research*, 88, 2693–2703, doi:10.1029/JC088iC04p02693, 1983.

575 Jouzel J., et al.: Validity of the temperature reconstruction from water isotopes in ice
576 cores, *Journal of Geophysical Research*, 102, 26471–26487,
577 doi:10.1029/97JC01283, 1997.

578 Jouzel J., Vimeux F., Caillon N., Delaygue G., Hoffman G., Masson-Delmotte V., and
579 Parrenin F.: Magnitude of isotope/temperature scaling for interpretation of central
580 Antarctic ice cores, *Journal of Geophysical Research*, 108, 1–6,
581 doi:10.1029/2002JD002677, 2003.

582 Kaempfer T. U., and Schneebeli M. Observation of isothermal metamorphism of new
583 snow and interpretation as a sintering process, *Journal of Geophysical Research*,
584 112(D24), 1–10, doi:10.1029/2007JD009047, 2007.

585 Krinner G. and Werner M.: Impact of precipitation seasonality changes on isotopic
586 signals in polar ice cores: A multi-model analysis, *Earth and Planetary Science*
587 *Letters*, 216, 525–538, doi:10.1016/S0012-821X(03)00550-8, 2003.

588 Lorius C., Merlivat L., Jouzel J., and Pourchet M.: A 30,000-yr isotope climatic record
589 from Antarctica ice, *Nature*, 280, 644–648, doi:10.1038/280644a0, 1979.

590 Löwe H., Spiegel J. K., and Schneebeli M.: Interfacial and structural relaxations of
591 snow under isothermal conditions, *Journal of Glaciology*, 57, 499-510,
592 doi:10.3189/002214311796905569, 2011.

593 Masson-Delmotte V., Steen-Larsen H. C., Ortega P., Swingedouw D., Popp T., Vinther
594 B. M., Oerter H., Sveinbjornsdottir A. E., Gudlaugsdottir H., Box J. E., Falourd S.,
595 Fettweis X., Gallee H., Garnier E., Jouzel J., Landais A., Minster B., Paradis N.,
596 Orsi A., Risi C., Werner M., and White J. W. C.: Recent changes in north-west
597 Greenland climate documented by NEEM shallow ice core data and simulations,
598 and implications for past temperature reconstructions, *The Cryosphere*, 9, 1481-
599 1504, doi:10.5194/tc-9-1481-2015, 2015.

600 Merlivat L. and Jouzel J.: Global climatic interpretation of the deuterium-oxygen 18
601 relationship for precipitation, *Journal of Geophysical Research*, 84, 5029–5033,
602 doi:10.1029/JC084iC08p05029, 1979.

603 Neumann T. A.: Effects of firn ventilation on geochemistry of polar snow, PhD thesis,
604 University of Washington, Washington, USA, 2003.

605 Neumann T. A. and Waddington E. D.: Effects of firn ventilation on isotopic exchange,
606 *Journal of Glaciology*, 50, 183–194, 2004.

607 Neumann T. A., Albert M. R., Lomonaco R., Engel C., Courville Z., and Perron F.:
608 Experimental determination of snow sublimation rate and stable-isotopic exchange,
609 *Annals of Glaciology*, 49, 1–6, doi:10.3189/172756408787814825, 2008.

610 Otsu N.: A Threshold Selection Method from Gray-Level Histograms, *IEEE*
611 *Transactions on Systems Man and Cybernetics*, 9, 62–66, 1979.

612 Persson A., Langen P. L., Ditlevsen P., and Vinther B. M.: The influence of
613 precipitation weighting on interannual variability of stable water isotopes in
614 Greenland, *Journal of Geophysical Research – Atmosphere*, 116, 1-13,
615 doi:10.1029/2010JD015517, 2011.

616 Petit J. R., et al.: Climate and atmospheric history of the past 420,000 years from the
617 Vostok ice core, Antarctica, *Nature*, 399, 429–436, doi:10.1038/20859, 1999.

618 Pinzer B. R. and Schneebeli M.: Snow metamorphism under alternating temperature
619 gradients: Morphology and recrystallization in surface snow, *Geophysical Research*
620 *Letters*, 36, doi:10.1029/2009GL039618, 2009.

621 Pinzer B. R., Schneebeli M., and Kaempfer T. U.: Vapor flux and recrystallization
622 during dry snow metamorphism under a steady temperature gradient as observed by
623 time-lapse microtomography, *The Cryosphere*, 6, 1141–1155, doi:10.5194/tc-6-
624 1141-2012, 2012.

625 Ramseier R. O: Self-diffusion of tritium in natural and synthetic ice monocrystals,
626 *Journal of Applied Physics*, 38, 2553-2556, 1967.

627 Ritter F., Steen-Larsen H. C., Werner M., Masson-Delmotte V., Orsi A., Behrens M.,
628 Birnbaum G., Freitag J., Risi C., and Kipfstuhl S.: Isotopic exchange on the diurnal
629 scale between near-surface snow and lower atmospheric water vapor at Kohnen
630 station, East Antarctica, *The Cryosphere Discussion*, doi:10.5194/tc-2016-4, in
631 review, 2016.

632 Schleef S., Jaggi M., Löwe H., and Schneebeli M.: Instruments and Methods: An
633 improved machine to produce nature-identical snow in the laboratory, *Journal of*
634 *Glaciology*, 60, 94–102, 2014.

635 Sjolte J., Hoffmann G., Johnsen S. J., Vinther B. M., Masson-Delmotte V., and Sturm
636 C.: Modeling the water isotopes in Greenland precipitation 1959-2001 with the

637 meso-scale model remo-iso, *Journal of Geophysical Research*, 116, 1-22,
638 doi:10.1029/2010JD015287, 2011.

639 Sokratov S. A. and Golubev V. N.: Snow isotopic content change by sublimation.
640 *Journal of Glaciology*, 55(193), 823-828, doi:10.3189/002214309790152456, 2009.

641 Steen-Larsen H. C., Masson-Delmotte V., Sjolte J., Johnsen S. J., Vinther B. M., Breon
642 F. M., Clausen H. B., Dahl-Jensen D., Falourd S., Fettweis X., Gallee H., Jouzel J.,
643 Kageyama M., Lerche H., Minster B., Picard G., Punge H. J., Risi C.,
644 Salas D., Schwander J., Steffen K., Sveinbjörnsdóttir A. E., Svensson A., and
645 White J.: Understanding the climatic signal in the water stable isotope records from
646 the neem shallow firn/ice cores in northwest Greenland, *Journal of Geophysical
647 Research - Atmosphere*, 116, 1–20, doi:10.1029/2010JD014311, 2011.

648 Steen-Larsen H. C., Johnsen S. J., Masson-Delmotte V., Stenni B., Risi C., Sodemann
649 H., Balslev-Clausen D., Blunier T., Dahl-Jensen D., Ellehøj M. D., Falourd S.,
650 Grindsted A., Gkinis V., Jouzel J., Popp T., Sheldon S., Simonsen S. B., Sjolte J.,
651 Steffensen J. P., Sperlich P., Sveinbjörnsdóttir A. E., Vinther B. M., and Whiste J.
652 W. C.: Continuous monitoring of summer surface water vapor isotopic composition
653 above the Greenland Ice Sheet, *Atmospheric Chemistry and Physics*, 13, 4815–
654 4828, doi: 10.5194/acp-13-4815-2013, 2013.

655 Steen-Larsen H. C., Masson-Delmotte V., Hirabayashi M., Winkler R., Satow K., Prié
656 F., Bayou N., Brun E., Cuffey K. M., Dahl-Jensen D., Dumont M., Guillevic M.,
657 Kipfstuhl S., Landais A., Popp T., Risi C., Steffen K., Stenni B., and
658 Sveinbjörnsdóttir A. E.: What controls the isotopic composition of Greenland
659 surface snow?, *Climate of the Past*, 10, 377–392, doi:10.5194/cp-10-377-2014.,
660 2014a.

661 Steen-Larsen H. C., Sveinbjörnsdóttir A. E., Peters A. J., Masson-Delmotte V.,
662 Guishard M. P., Hsiao G., Jouzel J., Noone D., Warren J. K., and White J. W. C.:
663 Climatic controls on water vapor deuterium excess in the marine boundary layer of
664 the North Atlantic based on 500 days of in situ, continuous measurements,
665 Atmospheric Chemistry and Physics, 14, 7741-7756, doi:10.5194/acp-14-7741-
666 2014., 2014b.

667 Sturm M. and Johnson J. B.: Natural convection in the subarctic snow cover, Journal of
668 Geophysical Research, 96, 11657–11671, doi:10.1029/91JB00895, 1991.

669 Town M. S., Warren S. G., Walden V. P., and Waddington E. D.: Effect of atmospheric
670 water vapor on modification of stable isotopes in near-surface snow on ice sheets,
671 Journal of Geophysical Research-Atmosphere, 113, 1-16,
672 doi:10.1029/2008JD009852, 2008.

673 Van der Wel G., Fischer H., Oerter H., Meyer H., and Meijer H. A. J.: Estimation and
674 calibration of the water isotope differential diffusion length in ice core records, The
675 Cryosphere Discussion, 9, 927-973, doi:10.5194/tc-9-1601-2015, 2015

676 Waddington E. D., Cunningham J., and Harder S. L.: The effects of snow ventilation on
677 chemical concentrations, in: Chemical Exchange Between the Atmosphere and
678 Polar Snow, edited by: Wolff, E. W. and Bales, R. C., Springer, Berlin, NATO ASI
679 Series, 43, 403–452, 1996.

680 Waddington E. D., Steig E. J., and Neumann T. A.: Using characteristic times to assess
681 whether stable isotopes in polar snow can be reversibly deposited. Annals of
682 Glaciology, 35, 118–124, doi:10.3189/172756402781817004, 2002.

683 Werner M., Langebroek P. M., Carlsen T., Herold M., and Lohmann G.: Stable water
684 isotopes in the ECHAM5 general circulation model: Toward high-resolution

685 isotope modeling on a global scale, *Journal of Geophysical Research Atmosphere*,
686 116, D15109, doi:10.1029/2011JD015681, 2011.

687 White J. W., Barlow L. K., Fisher D., Grootes P., Jouzel J., Johnsen S. J., Stuiver M.,
688 and Clausen H.: The climate signal in the stable isotopes of snow from Summit,
689 Greenland: Results of comparisons with modern climate observations, *Journal of*
690 *Geophysical Research*, 102, 26425–26439, doi:10.1029/97JC00162, 1997.

691 Zermatten E., Schneebeli M., Arakawa H., and Steinfeld A.: Tomography-based
692 determination of porosity, specific area and permeability of snow and comparison
693 with measurements, *Cold Regions Science and Technology*, 97, 33–40,
694 doi:10.1016/j.coldregions.2013.09.013, 2014.

695

696

697 **Table 1:** Morphological properties and flow characteristics of the experimental runs:
698 snow density (ρ), porosity (ε), specific surface area per unit mass (SSA), mean pore
699 space diameter (d_{mean}), superficial velocity in snow (u_D), corresponding Reynolds
700 number ($\text{Re} = d_{\text{mean}} \cdot u_D / \nu_{\text{air}}$), average inlet temperature of the humidifier and at the inlet
701 ($T_{\text{in,mean}}$), average outlet temperature at the outlet ($T_{\text{out,mean}}$), and average temperature
702 gradient (∇T_{ave}). Experiment (1) corresponds to the isothermal conditions; Experiment
703 (2) to air warming; and Experiment (3) to air cooling in the snow sample.

704

	ρ kg m ⁻³	ε –	SSA m ² kg ⁻¹	d_{mean} mm	u_D m s ⁻¹	Re –	$T_{\text{in,mean}}$ °C	$T_{\text{out,mean}}$ °C	∇T_{ave} K m ⁻¹
Experiment (1)	201.74	0.78	28.0	0.39	0.03	0.76	-15.5	-15.5	–
Experiment (2)	201.74	0.78	29.7	0.36	0.03	0.70	-15.4	-14.0	+47
Experiment (3)	220.08	0.76	27.2	0.37	0.031	0.74	-12.3	-14.1	-60

705

706 **Table 2:** $\delta^{18}\text{O}$ in the vapor in the humidifier ($\delta^{18}\text{O}_{\text{hum}}$) and of the snow in the sample
 707 holder ($\delta^{18}\text{O}_s$) at the beginning ($t = 0$) and end ($t = \text{end}$) of each experiment and the final
 708 $\delta^{18}\text{O}$ content of the snow in the sample holder at the inlet ($z = 0$ mm) and outlet ($z = 30$
 709 mm). Experiment (1) corresponds to the isothermal conditions; Experiment (2) to air
 710 warming; and Experiment (3) to air cooling in the snow sample.

711

	$\delta^{18}\text{O}_{\text{hum}}$		$\delta^{18}\text{O}_{s, t=0}$	$\delta^{18}\text{O}_{s, t=\text{end}}$	
	%o			%o	
	$t = 0$	$t = \text{end}$		$z = 0$ mm	$z = 30$ mm
Experiment (1)	-68.2	-67.5	-10.97	-17.75	-15.72
Experiment (2)	-66.3	-66.1	-11.94	-19.60	-16.60
Experiment (3)	-62.8	-62.2	-10.44	-25.53	-15.00

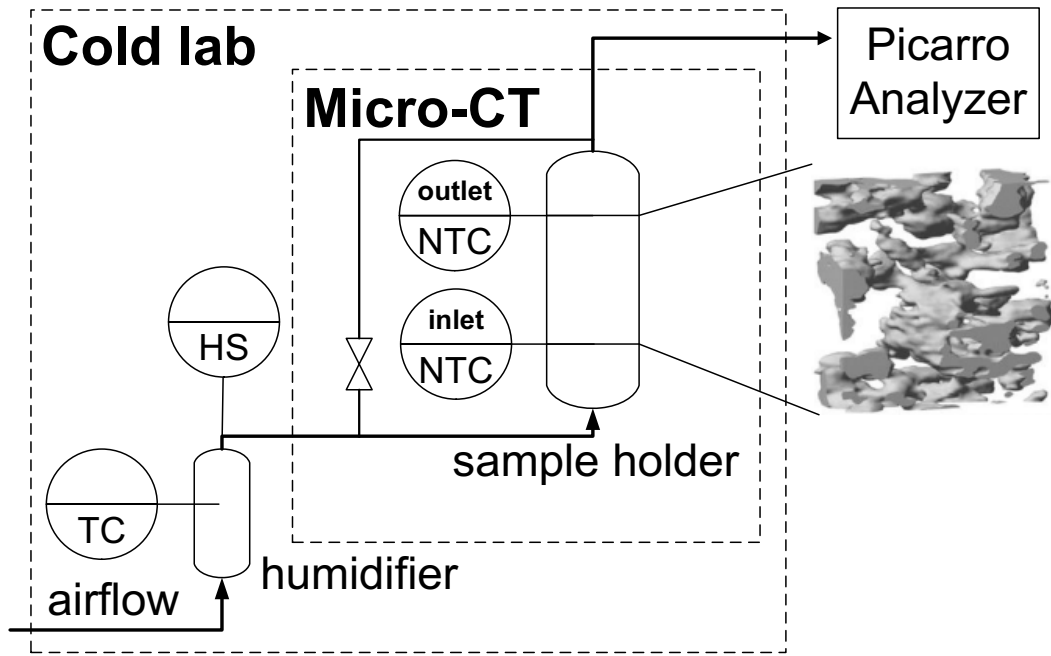
712

713 **Figure captions**

714 **Fig. 1.** Schematic of the experimental setup. A thermocouple (TC) and a humidity
715 sensor (HS) inside the humidifier measured the the mean temperature and
716 humidity of the airflow. Two thermistors (NTC) close to the snow surface
717 measured the inlet and outlet temperature of the airflow (Ebner et al., 2014).
718 The Picarro Analyzer measured the isotopic composition $\delta^{18}\text{O}$ of the outlet
719 flow. Inset: 3D structure of $110 \times 42 \times 110$ voxels ($2 \times 0.75 \times 2 \text{ mm}^3$)
720 obtained by the μCT .

721 **Fig. 2.** Temporal isotopic composition of $\delta^{18}\text{O}$ of the outflow for each of the
722 experimental runs. The spikes in the $\delta^{18}\text{O}$ were due to small temperature
723 changes in the cold laboratory (Ebner et al., 2014). Exp. (1) corresponds to
724 the isothermal conditions; Exp. (2) to air warming; and Exp. (3) to air
725 cooling in the snow sample. The higher the recrystallization rate of the snow
726 the slower the adaption of $\delta^{18}\text{O}$ of the outlet air to the inlet air. The
727 illustration in the lower right corner shows the relation between $\delta^{18}\text{O}$ of the
728 initial snow, inlet, and outlet of the air.

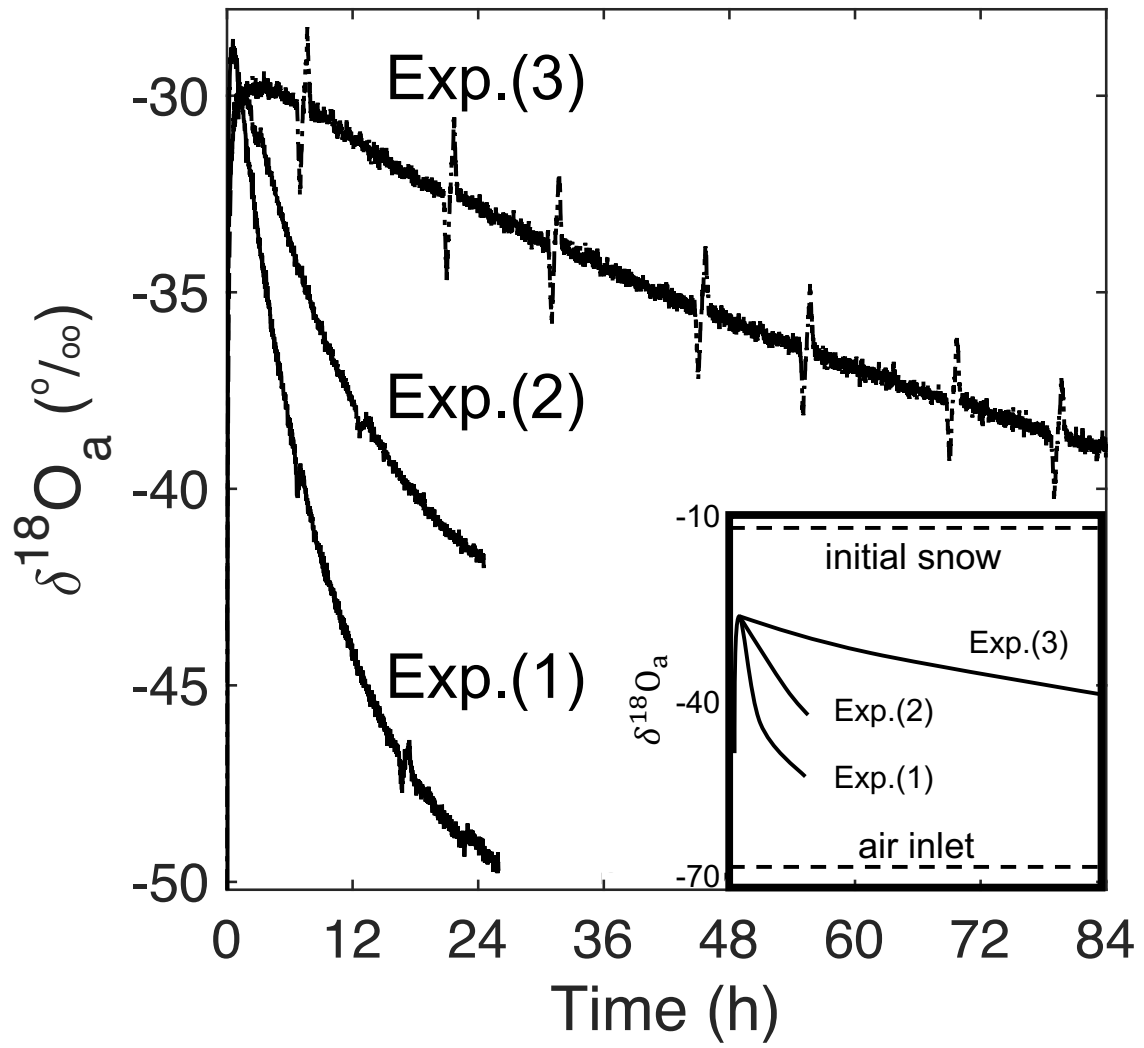
729 **Fig. 3.** Spatial isotopic composition of $\delta^{18}\text{O}$ of the snow sample at the beginning (t
730 $= 0$) and at the end ($t = \text{end}$) for each experiment. The air entered at $z = 0$
731 mm and exited at $z = 30$ mm. Exp. (1) corresponds to the isothermal
732 conditions; Exp. (2) to air warming; and Exp. (3) to air cooling in the snow
733 sample.



734

735

Fig. 1

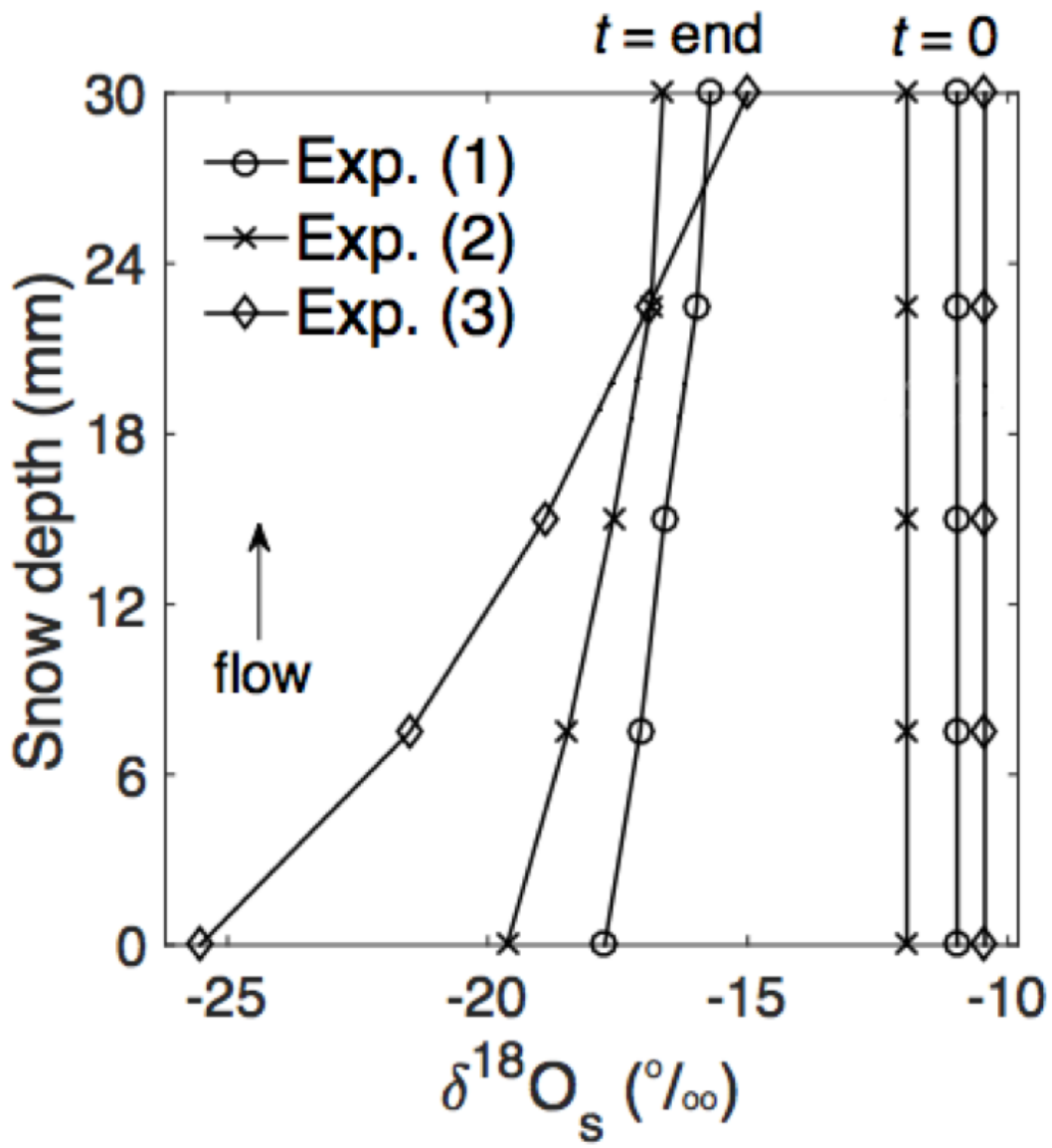


736

737

738

Fig. 2



739

740

Fig. 3